Enhanced Electrocatalytic Activities of In Situ Produced Pd/S/N Doped Carbon on Oxygen Reduction and Hydrogen Evolution Reactions

Malenahalli Halappa Naveen [a], Yuanhui Huang [a], Sunitha Bisalere Kantharajappa [a], Kyeong-Deok Seo [a], Deog-Su Park [b], and Yoon-Bo Shim*[a b]

[a] Department of Chemistry, Pusan National University, Busan, 46241, Republic of Korea.

[b] Institute of BioPhysio Sensor Technology, Pusan National University, Busan, 46241, Republic of Korea.

*Corresponding Author

E-mail: ybshim@pusan.ac.kr

KEYWORDS: Coordination polymer; Pd-rubeanic acid; S and N doping; doped Palladium carbon; Electrocatalysis

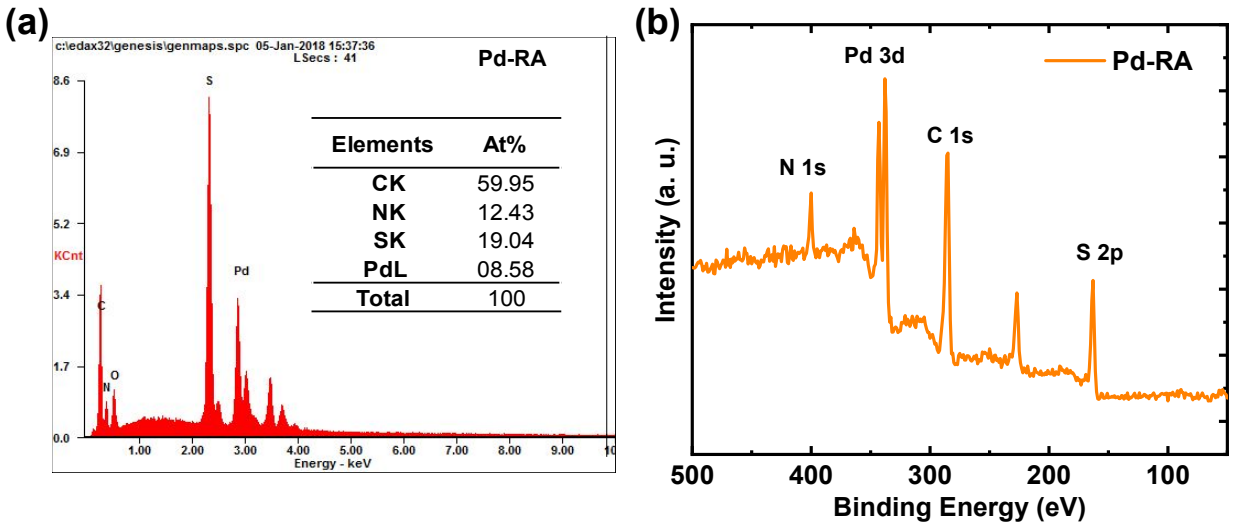

Figure S1. (a) EDX and (b) XPS survey spectra for Pd-RA sample.

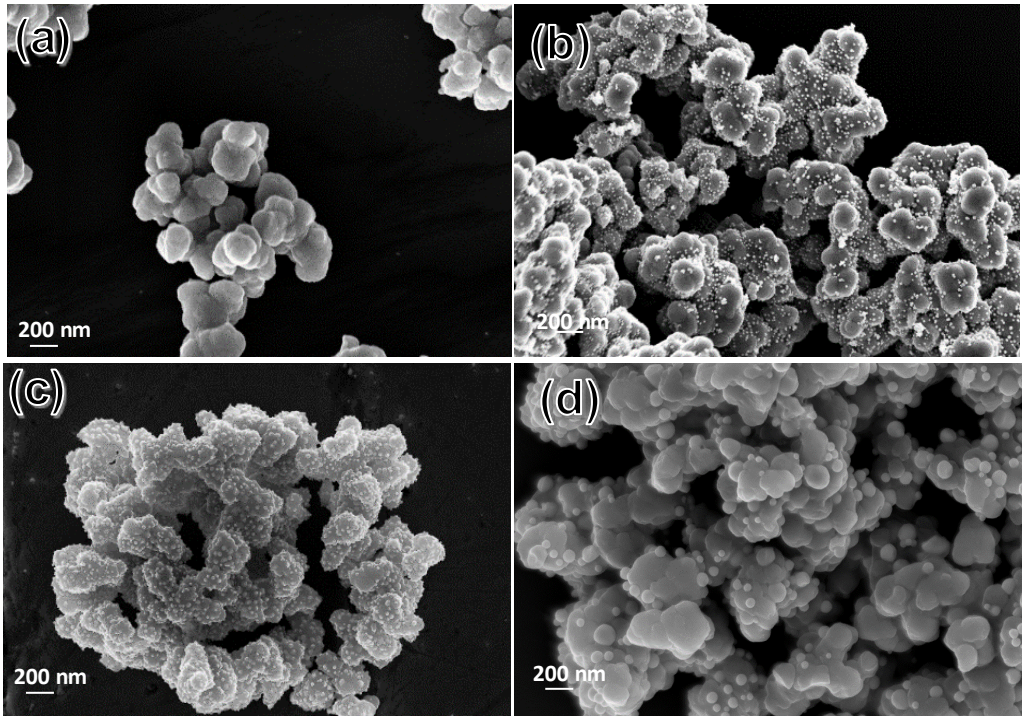

Figure S2. FESEM images for PdSNC prepared at different carbonization temperature (a) 400 °C, (b) 500 °C, (c) 600 °C, and (d) 700 °C.

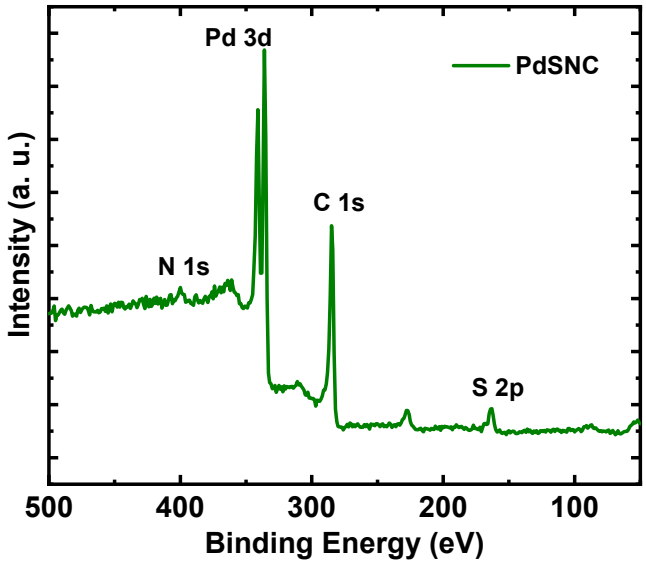

Figure S3. XPS survey spectra for PdSNC preraed at 600 °C.

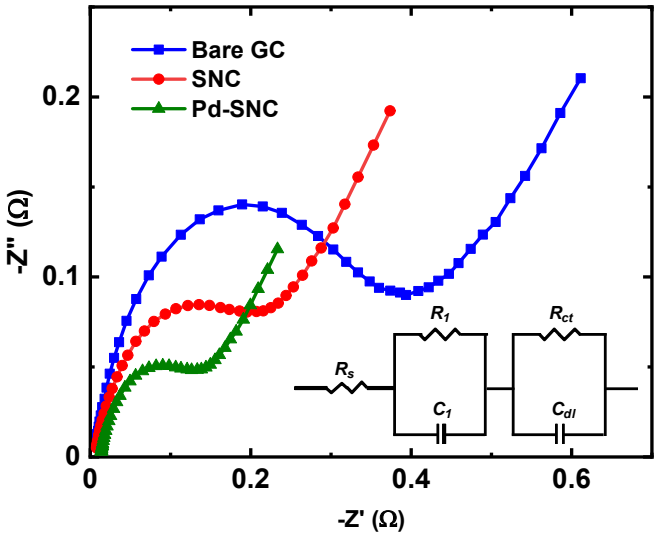

Figure S4. EIS for GC, SNC, and PdSNC. Inset is the equivalent circuit used for fitting.

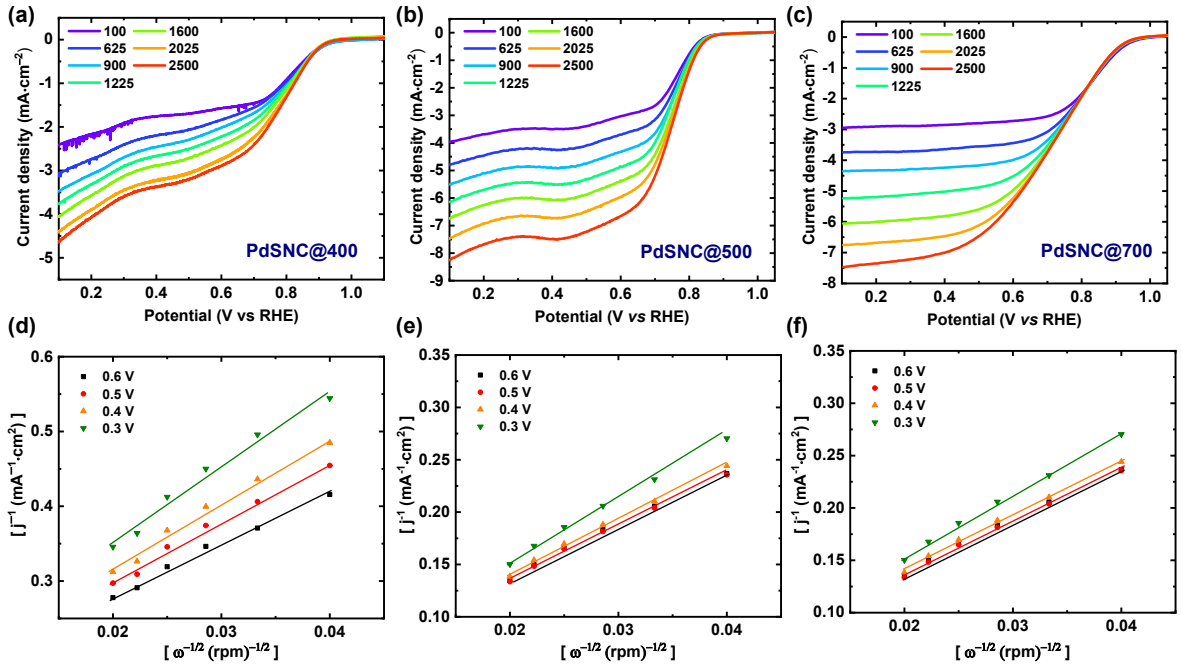

Figure S5. RDE plots at different rpm for PdSNC prepared at 400 °C, 500 °C and 700 °C (a, b and c) and corresponding K-L plots (d, e, and f).

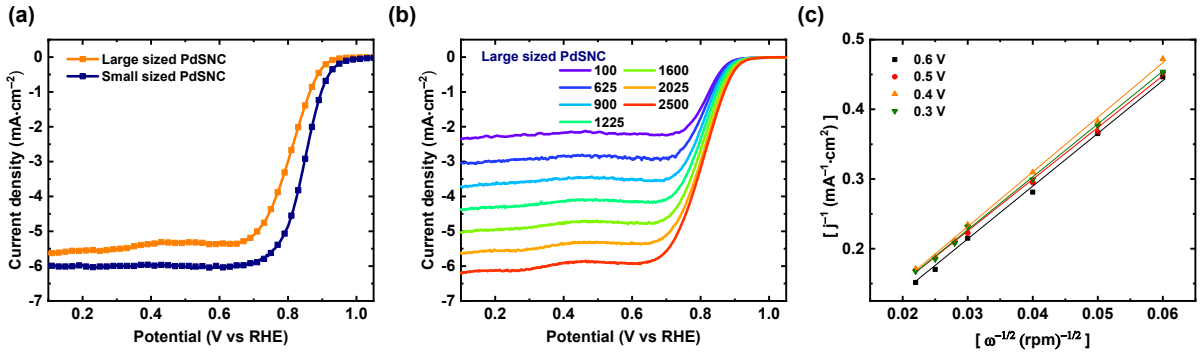

Figure S6. (a) LSV curves for large and small sized PdSNC. (b and c) RDE and K-L plot at different rpm for large sized PdSNC.

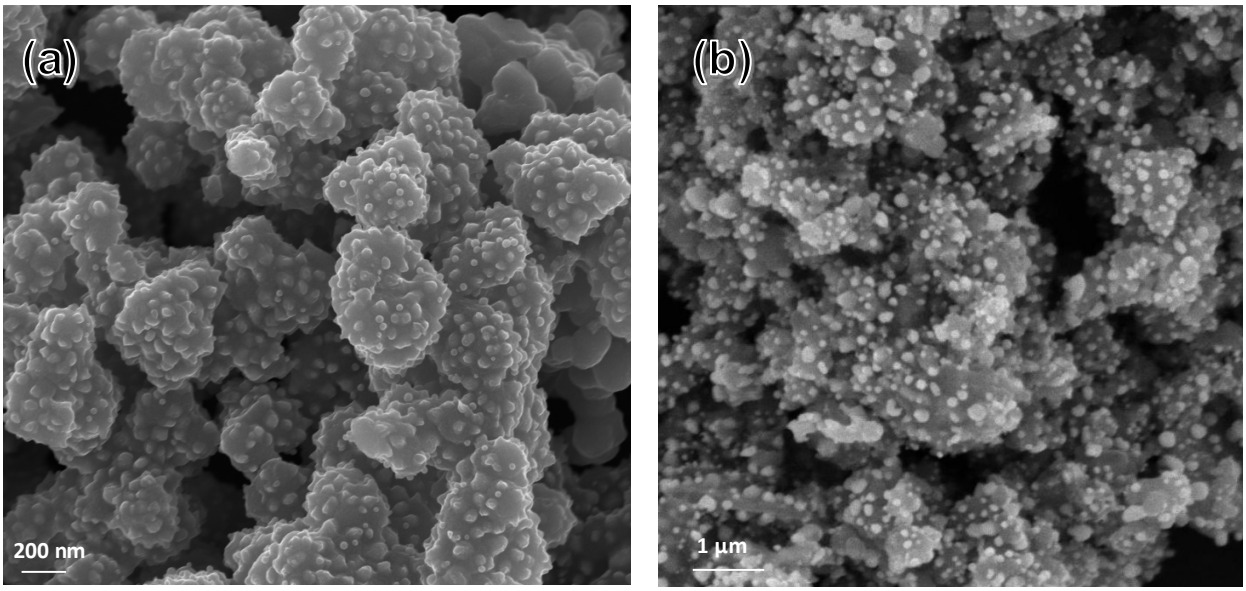

Figure S7. (a and b) FESEM images of small and large sized PdSNC after calcination at 600 °C.

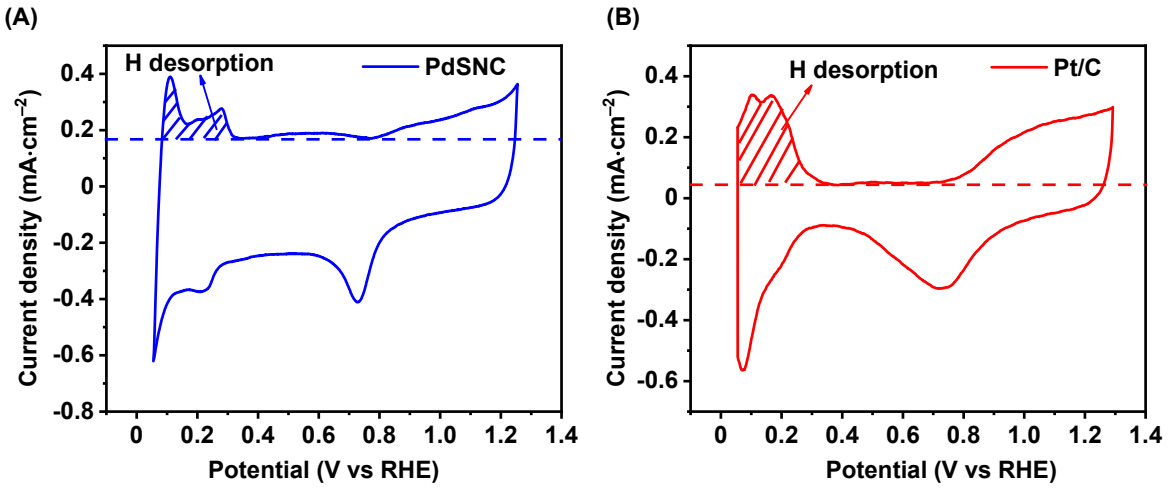

Figure S8. CVs of PdSNC and PtC in N_2 gas saturated 0.5 M H_2SO_4 at a scan rate of 50 $mV \cdot s^{-1}$. The electrochemical surface area (ECSA) of the PdSNC and PtC was calculated and it was found to be 0.372 cm^2 and 0.445 cm^2 respectively based on the H adsorption/desorption method.

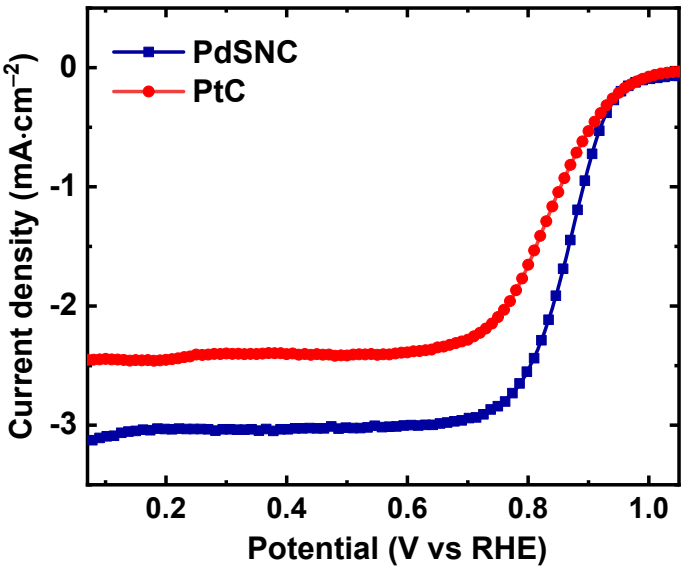

Figure S9. LSV curves for PdSNC and PtC were recorded at 1600 rpm in O_2 saturated 0.1 M KOH at a scan rate of 5 mV·s^{-1}. For area-specific activity comparison, the ORR current density is normalized with ECSA. This result suggested that the better catalytical activity for the PdSNC in comparison with PtC catalyst.

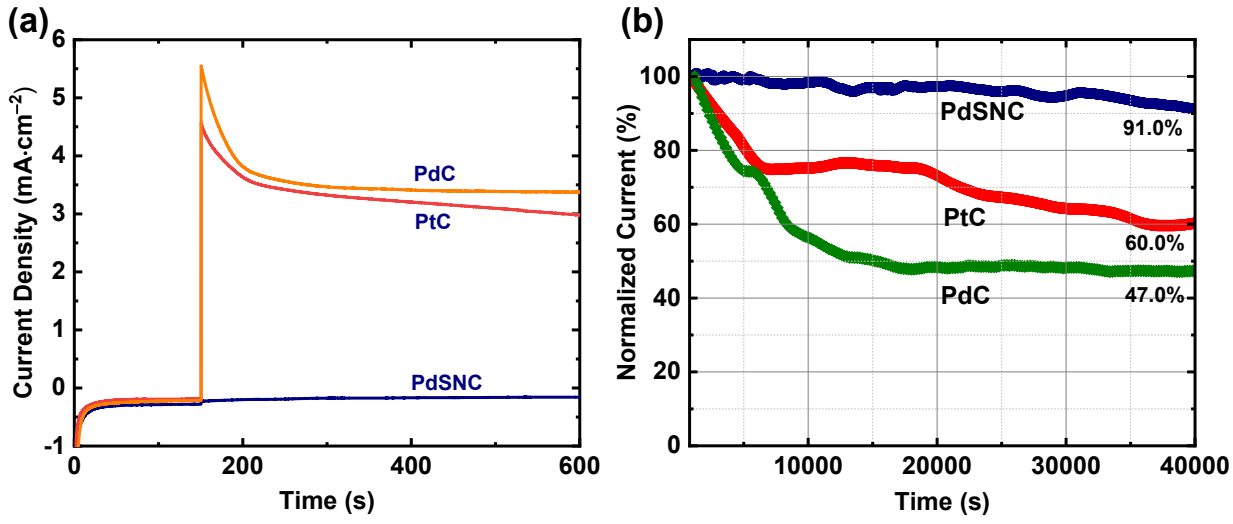

Figure S10. (a) Chronoamperometric responses of PdSNC, PtC and PdC with injection of 3 M methanol in O_2 saturated 0.1 M KOH solution. (b) Stability comparison for PdSNC, PtC and PdC catalysts.

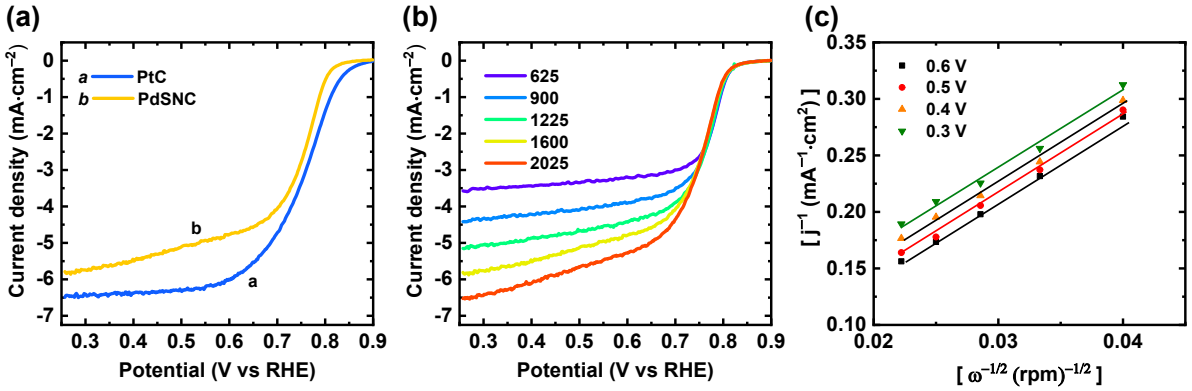

Figure S11. (a) LSVs comparison between PdSNC and PtC at 1600 rpm (b) ORR polarization curves at different rpm for PdSNC in 0.1 M $HClO_4$ solution and (c) corresponding K-L plot.

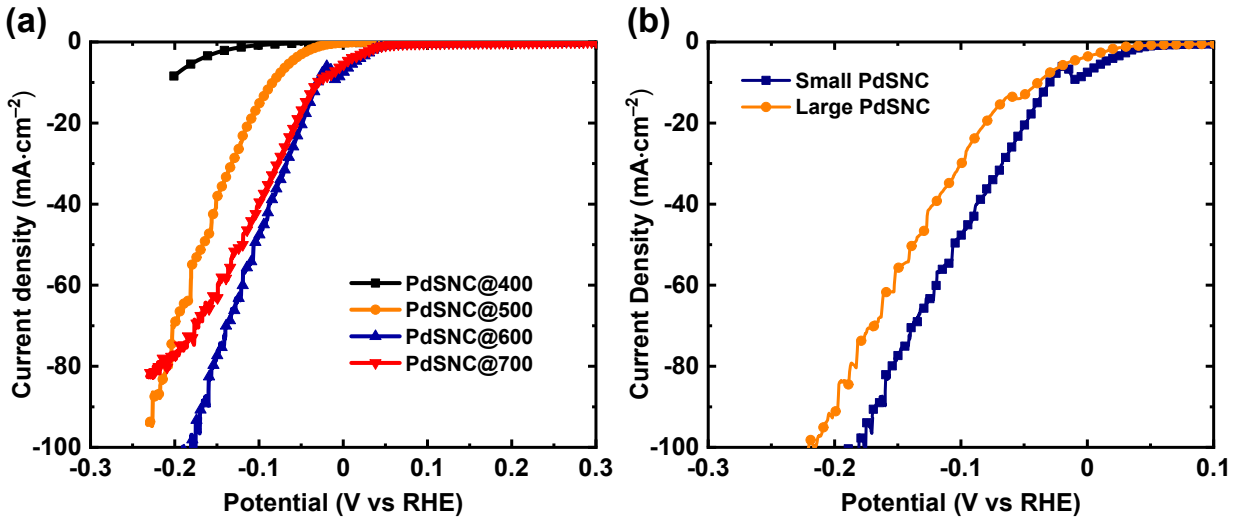

Figure S12. (a) HER comparison for of PdSNC prepared at different carbonization temperature and (b) HER LSV curves of small and large sized PdSNC samples.

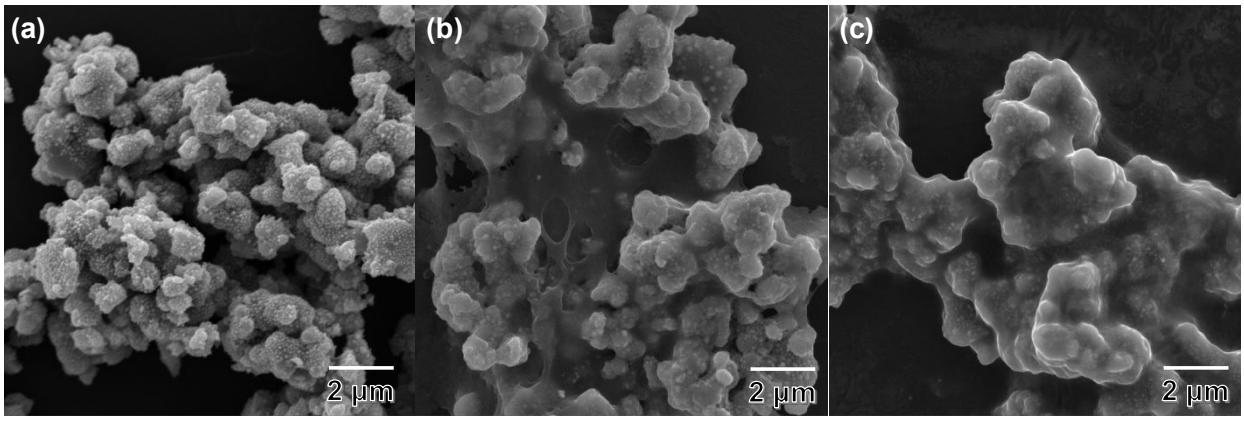

Figure S13. SEM images of PdSNC (a) before (b) after ORR (c) after HER test performed.

The shade light on the structural stability of Pd NPs after the ORR and HER test, we have characterized their surface by SEM measurements. As shown in Figure S13, the overall morphology of PdSNC was remained intact and the size of Pd NPs also not altered, revealing its structural robustness due to the strong support from the S and N atoms in the carbon network. The presence of the Nafion layer is noticeable in SEM images, which is used as a binder to keep the catalysts on the RDE when the electrode is rotated.

Table S1. Comparison of ORR performance in 0.1M KOH of PdSNC with other Pd based electrocatalysts

Electrocatalyst	**E_{onset} (V vs RHE)**	**$E_{1/2}$ (V vs RHE)**	**References**
PtC	**1.020**	**0.830**	**This work**
PdC	**0.900**	**0.791**	
SNC	**0.857**	**0.786**	
PdSNC	**1.060**	**0.867**	
Pd_3Pb intermetallic compound	---	0.93	[3]
Pd−Fe@PdC	---	0.866	[4]
Pd@PdO-Co_3O_4	---	0.90	[5]
fct-PdFe@Pd	0.97	0.830	[6]

$Au@Pd_{1.0}$	---	0.85	[7]
Pt@Pd NFs/rGO	0.91	0.82	[8]
Pd@PtNi core−shell nanoflower	---	0.87	[9]
Au-NWs@Pd0.1@PEI	---	0.90	[10]
PdCuTiAl	---	0.87	[11]
Pd@PdPt	---	0.91	[12]
Pd@NiO-x/C	---	0.87	[13]
Pd nanoparticles/nitrogen doped graphene	---	0.85	[14]
$Ni@Pd_3/C$	0.98	0.860	[15]

Table S2. Comparison of HER performance for PdSNC with other selected electrocatalysts

Electrocatalyst	**Electrolyte**	**Overpotential (mV) at 10 mA/cm²**	**Tafel slope ($mV \cdot dec^{-1}$)**	**References**
PtC	**0.5 M H_2SO_4**	**27**	**20**	**This work**
PdC	**0.5 M H_2SO_4**	**96**	**82**	
SNC	**0.5 M H_2SO_4**	**203**	**-**	
PdSNC	**0.5 M H_2SO_4**	**30**	**56**	
PdCu@Pd NCs	0.5 M H_2SO_4	65	35	[16]
FeP NPs@NPC	0.5 M H_2SO_4	130	67	[17]

FLNPC@MoP-NC/MoP-C/CC	0.5 M H_2SO_4	74	50	[18]
$Cu_{2-x}S$@Ru NPs	0.5 M H_2SO_4	129	51	[19]
CoPd@NC	0.5 M H_2SO_4	80	31	[20]
$NiCo_2S_4$/Pd	0.5 M H_2SO_4	87	70	[21]
P-Mo_2C@C nanowires	0.5 M H_2SO_4	89	42	[22]
Co_9S_8-30@MoS_x/CC	0.5 M H_2SO_4	98	64.8	[23]
Mo/MoC_{1-x}	0.5 M H_2SO_4	75	81	[24]
$MoSe_2$	0.5 M H_2SO_4	100	63	[25]
Pd-Cu-S	0.5 M H_2SO_4	58	35	[26]
Fe1.89Mo4.11O7	0.5 M H_2SO_4	125	47	[27]

References:

1. Chen, X.; Granda-Marulanda, L. P.; McCrum, I. T.; Koper, M. T. M., Adsorption processes on a Pd monolayer-modified Pt(111) electrode. *Chemical Science* **2020,** *11* (6), 1703-1713.
2. Woods, R., *Electroanalytical Chemistry*. Marcel Dekker: New York 1976; Vol. 9.
3. Cui, Z.; Chen, H.; Zhao, M.; DiSalvo, F. J., High-Performance Pd3Pb Intermetallic Catalyst for Electrochemical Oxygen Reduction. *Nano Lett.* **2016,** *16* (4), 2560-2566.
4. Xiong, Y.; Yang, Y.; DiSalvo, F. J.; Abruña, H. D., Pt-Decorated Composition-Tunable Pd–Fe@Pd/C Core–Shell Nanoparticles with Enhanced Electrocatalytic Activity toward the Oxygen Reduction Reaction. *J. Am. Chem. Soc.* **2018,** *140* (23), 7248-7255.
5. Li, H.-C.; Zhang, Y.-J.; Hu, X.; Liu, W.-J.; Chen, J.-J.; Yu, H.-Q., Metal-Organic Framework Templated Pd@PdO-Co3
O4

Nanocubes as an Efficient Bifunctional Oxygen Electrocatalyst. *Adv. Energy Mater.* **2018,** *8* (11), 1702734.
6. Maiti, K.; Balamurugan, J.; Peera, S. G.; Kim, N. H.; Lee, J. H., Highly Active and Durable Core–Shell fct-PdFe@Pd Nanoparticles Encapsulated NG as an Efficient Catalyst for Oxygen Reduction Reaction. *ACS Applied Materials & Interfaces* **2018,** *10* (22), 18734-18745.
7. Zong, Z.; Xu, K.; Li, D.; Tang, Z.; He, W.; Liu, Z.; Wang, X.; Tian, Y., Peptide templated Au@Pd core-shell structures as efficient bi-functional electrocatalysts for both oxygen reduction and hydrogen evolution reactions. *J. Catal.* **2018,** *361*, 168-176.
8. Lin, X.-X.; Wang, A.-J.; Fang, K.-M.; Yuan, J.; Feng, J.-J., One-Pot Seedless Aqueous Synthesis of Reduced Graphene Oxide (rGO)-Supported Core–Shell Pt@Pd Nanoflowers as Advanced Catalysts for Oxygen Reduction and Hydrogen Evolution. *ACS Sustainable Chemistry & Engineering* **2017,** *5* (10), 8675-8683.
9. Liu, S.; Wang, Y.; Liu, L.; Li, M.; Lv, W.; Zhao, X.; Qin, Z.; Zhu, P.; Wang, G.; Long, Z.; Huang, F., One-pot synthesis of Pd@PtNi core-shell nanoflowers supported on the multi-walled carbon nanotubes with boosting activity toward oxygen reduction in alkaline electrolyte. *J. Power Sources* **2017,** *365*, 26-33.
10. Xue, Q.; Bai, J.; Han, C.; Chen, P.; Jiang, J.-X.; Chen, Y., Au Nanowires@Pd-Polyethylenimine Nanohybrids as Highly Active and Methanol-Tolerant Electrocatalysts toward Oxygen Reduction Reaction in Alkaline Media. *Acs Catal* **2018,** *8* (12), 11287-11295.
11. Chen, X.; Si, C.; Wang, Y.; Ding, Y.; Zhang, Z., Multicomponent platinum-free nanoporous Pd-based alloy as an active and methanol-tolerant electrocatalyst for the oxygen reduction reaction. *Nano Research* **2016,** *9* (6), 1831-1843.
12. Liu, Y.; Liu, S.; Che, Z.; Zhao, S.; Sheng, X.; Han, M.; Bao, J., Concave octahedral Pd@PdPt electrocatalysts integrating core–shell, alloy and concave structures for high-efficiency oxygen reduction and hydrogen evolution reactions. *J. Mater. Chem. A* **2016,** *4* (42), 16690-16697.
13. Feng, Y.; Yang, C.; Fang, W.; Huang, B.; Shao, Q.; Huang, X., Anti-poisoned oxygen reduction by the interface modulated Pd@NiO core@shell. *Nano Energy* **2019,** *58*, 234-243.
14. Kabir, S.; Serov, A.; Artyushkova, K.; Atanassov, P., Nitrogen-Doped Three-Dimensional Graphene-Supported Palladium Nanocomposites: High-Performance Cathode Catalysts for Oxygen Reduction Reactions. *Acs Catal* **2017,** *7* (10), 6609-6618.
15. Jiang, J.; Gao, H.; Lu, S.; Zhang, X.; Wang, C.-Y.; Wang, W.-K.; Yu, H.-Q., Ni–Pd core–shell nanoparticles with Pt-like oxygen reduction electrocatalytic performance in both acidic and alkaline electrolytes. *J. Mater. Chem. A* **2017,** *5* (19), 9233-9240.
16. Li, J.; Li, F.; Guo, S.-X.; Zhang, J.; Ma, J., PdCu@Pd Nanocube with Pt-like Activity for Hydrogen Evolution Reaction. *ACS Applied Materials & Interfaces* **2017,** *9* (9), 8151-8160.
17. Pu, Z.; Amiinu, I. S.; Zhang, C.; Wang, M.; Kou, Z.; Mu, S., Phytic acid-derivative transition metal phosphides encapsulated in N,P-codoped carbon: an efficient and durable hydrogen evolution electrocatalyst in a wide pH range. *Nanoscale* **2017,** *9* (10), 3555-3560.
18. Liu, B. C.; Li, H.; Cao, B.; Jiang, J. N.; Gao, R.; Zhang, J., Few Layered N, P Dual-Doped Carbon-Encapsulated Ultrafine MoP Nanocrystal/MoP Cluster Hybrids on Carbon Cloth: An Ultrahigh Active and Durable 3D Self-Supported Integrated Electrode for Hydrogen Evolution Reaction in a Wide pH Range. *Adv. Funct. Mater.* **2018,** *28* (30), 1801527.
19. Yoon, D.; Lee, J.; Seo, B.; Kim, B.; Baik, H.; Joo, S. H.; Lee, K., Cactus-Like Hollow Cu2-x S@Ru Nanoplates as Excellent and Robust Electrocatalysts for the Alkaline Hydrogen Evolution Reaction. *Small* **2017,** *13* (29), 1700052.

20. Chen, J.; Xia, G.; Jiang, P.; Yang, Y.; Li, R.; Shi, R.; Su, J.; Chen, Q., Active and Durable Hydrogen Evolution Reaction Catalyst Derived from Pd-Doped Metal–Organic Frameworks. *ACS Applied Materials & Interfaces* **2016,** *8* (21), 13378-13383.
21. Sheng, G.; Chen, J.; Li, Y.; Ye, H.; Hu, Z.; Fu, X.-Z.; Sun, R.; Huang, W.; Wong, C.-P., Flowerlike NiCo2S4 Hollow Sub-Microspheres with Mesoporous Nanoshells Support Pd Nanoparticles for Enhanced Hydrogen Evolution Reaction Electrocatalysis in Both Acidic and Alkaline Conditions. *ACS Applied Materials & Interfaces* **2018,** *10* (26), 22248-22256.
22. Shi, Z.; Nie, K.; Shao, Z.-J.; Gao, B.; Lin, H.; Zhang, H.; Liu, B.; Wang, Y.; Zhang, Y.; Sun, X.; Cao, X.-M.; Hu, P.; Gao, Q.; Tang, Y., Phosphorus-Mo2C@carbon nanowires toward efficient electrochemical hydrogen evolution: composition, structural and electronic regulation. *Energ Environ Sci* **2017,** *10* (5), 1262-1271.
23. Zhou, X.; Yang, X.; Hedhili, M. N.; Li, H.; Min, S.; Ming, J.; Huang, K.-W.; Zhang, W.; Li, L.-J., Symmetrical synergy of hybrid Co9S8-MoSx electrocatalysts for hydrogen evolution reaction. *Nano Energy* **2017,** *32*, 470-478.
24. Diao, J.; Yuan, W.; Su, Y.; Qiu, Y.; Guo, X., The Rational Design of Mo/MoC1− x Nanorods as Highly Active Electrocatalysts for Hydrogen Evolution Reaction. *Advanced Materials Interfaces* **2018,** *5* (13), 1800223.
25. Najafi, L.; Bellani, S.; Oropesa-Nunez, R.; Ansaldo, A.; Prato, M.; Castillo, A. E. D.; Bonaccorso, F., Engineered MoSe2-Based Heterostructures for Efficient Electrochemical Hydrogen Evolution Reaction. *Adv. Energy Mater.* **2018,** *8* (16), 1703212.
26. Xu, W.; Zhu, S.; Liang, Y.; Cui, Z.; Yang, X.; Inoue, A.; Wang, H., A highly efficient electrocatalyst based on amorphous Pd–Cu–S material for hydrogen evolution reaction. *J. Mater. Chem. A* **2017,** *5* (35), 18793-18800.
27. Hao, Z.; Yang, S.; Niu, J.; Fang, Z.; Liu, L.; Dong, Q.; Song, S.; Zhao, Y., A bimetallic oxide Fe1.89Mo4.11O7 electrocatalyst with highly efficient hydrogen evolution reaction activity in alkaline and acidic media. *Chemical Science* **2018,** *9* (25), 5640-5645.